Extending spin ice concepts to another geometry: The artificial triangular spin ice

L. A. S. Mól,[*] A. R. Pereira,[†] and W. A. Moura-Melo[‡]

Departamento de Física, Universidade Federal de Viçosa, Viçosa, 36570-000 Minas Gerais, Brazil
(Received 16 November 2011; revised manuscript received 10 April 2012; published 9 May 2012)

In this work, we propose and study a realization of an artificial spin-ice-like system in a triangular geometry, which, unlike square and kagome artificial spin ice, is not based on any real material. At each vertex of the lattice, the "icelike rule" dictates that three spins must point inward while the other three must point outward. We have studied the system's ground state and the lowest energy excitations as well as the thermodynamic properties of the system. Our results show that, despite fundamental differences in the vertex topologies as compared to the artificial square spin ice, in the triangular array the lowest energy excitations also behave like Nambu monopoles (two opposite monopoles connected by an energetic string). Indeed, our results suggest that the charge intensity of the monopoles may have a universal value while the string tension could be tuned by changing the system's geometry, probably allowing the design of systems with different string tensions. Our Monte Carlo findings suggest a phase transition in the Ising universality class where the mean distance between monopoles and antimonopoles increases considerably at the critical temperature. The differences in the vertex topologies seem to facilitate the experimental achievement of the system's ground state, thereby allowing a more detailed experimental study of the system's properties.

PACS number(s): 75.75.−c, 75.60.Ch, 75.60.Jk

I. INTRODUCTION

Geometrical frustration and fractionalization are key concepts in modern condensed matter theory. While the former is related to the impossibility of simultaneously minimizing the energy for all constituents of a system due to geometrical constraints, the latter is related to the appearance of collective excitations that carry only a fraction of the elementary constituents' properties. In some systems, these phenomena are closely related, as is the case of spin ice materials ($Dy_2Ti_2O_7$ and $Ho_2Ti_2O_7$).[1–7] There, due to a geometrical frustration, the energy is minimized by the appearance of the two-in/two-out ice rule, where at each vertex of a lattice two spins point inward and two outward. Violations of this rule are viewed thus as a fraction of a dipole,[1] since these collective excitations behave as magnetic monopoles, constituting the first example of fractionalization in three-dimensional (3D) materials.

With the aid of modern experimental techniques, mainly the capability to construct and manipulate nanostructured systems, artificial arrays with properties very similar to the spin ice material were recently built.[8–12] In particular, in an artificial frustrated 2D square array that mimics the spin ice behavior, the excitations above the ground state are viewed as a kind of Nambu magnetic monopoles,[13–17] since the end points of the energetic string behave like particles with magnetic charge, which leads to a Coulomb interaction (we remark that the Coulomb is a particular case of the Yukawa potential present in the Nambu calculations). Therefore, there is, of course, a huge amount of interest in accessing the ground state of the artificial square spin ice (ASSI) to test theoretical predictions concerning the appearance and behavior of monopole excitations.[18–21] However, demagnetization protocols[22–24] used so far were not able to drive the ASSI to its lowest energy state. Morgan *et al.*[16] successfully achieved what seems to be the thermalization of the ASSI during fabrication, although, they could not obtain a single ground-state domain.

In this work, we investigate whether the same fractionalization phenomenon manifested in the ASSI is also present in another artificial setting. We consider here a particular realization of an artificial spin ice in a triangular geometry. Unlike the square and kagome spin ice, our proposal is not based on any real material and was motivated by inquiring into what changes arise when the geometry of an artificially frustrated magnetic system is not the usual type for typical spin ices. By doing this, we have found that in the triangular geometry, the ground state is very likely to be easily obtained experimentally, which enables the experimental investigation of the existence and behavior of collective excitations above the ground state. In addition, we have found that the artificial triangular system also has collective excitations that can be described by a kind of Nambu monopole. As expected for a system which can be described by the same kind of excitation present in the ASSI, many similarities with ASSI were found. On the other hand, there are fundamental differences between the ASSI and the artificial triangular spin ice (ATSI), particularly with regard to the vertices' topologies. The existence of monopole-like excitations in the ATSI may also stimulate the search for other crystalline 3D materials where magnetic monopoles could appear.

II. THE ARTIFICIAL TRIANGULAR SPIN ICE

The study of spin-ice-like systems has somehow been restricted, until now, to two kinds of vertices: vertices with three spins, as in the kagome and brickwork lattices, and vertices with four spins, as in the natural spin ice materials ($Dy_2Ti_2O_7$ and $Ho_2Ti_2O_7$) and in the artificial square spin ice (ASSI). We may therefore ask what happens if we have a lattice with six spins per vertex instead of three or four. This is the basic question that motivated this study. To answer it, we have considered an array of elongated magnetic nanoparticles having a single domain pattern, such as those used to build the ASSI (Permalloy nanoislands), placed in a geometry such that the longest axis of each island points along the lines joining two vertices in a triangular lattice (see Fig. 1).
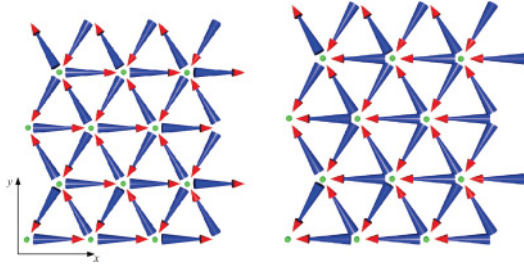
FIG. 1. (Color online) Left: A lattice with $L = 3$ in its ground state. The array proposed in this work has six spins in each vertex (small dots). The ice rule is now three in/three out. Right: By applying a strong magnetic field in the $-x$ direction the state shown here should be achieved, and by reversing the applied field the system should be driven to the ground state shown on the left side of the figure.

We have modeled the proposed system by replacing the magnetic moment of each island by a pointlike, Ising-like dipole ($\vec{S}_i$) that is constrained to point along the line that joins two vertices in the lattice, such that the interactions are expressed as follows:

$$H_{SI} = Da^3 \sum_{i \neq j} \left[\frac{\vec{S}_i \cdot \vec{S}_j}{r_{ij}^3} - \frac{3(\vec{S}_i \cdot \vec{r}_{ij})(\vec{S}_j \cdot \vec{r}_{ij})}{r_{ij}^5} \right], \quad (1)$$

where $D = \mu_0 \mu^2 / 4\pi a^3$ is the dipolar interaction coupling constant, a is the lattice spacing, and $\vec{r}_{ij}$ is a vector that connects islands i and j. In Fig. 1, we present a sketch of the system, where the vertices and the island's magnetic moments are shown.

We start our analysis by considering a single vertex and its six spins. It can be easily shown that it is energetically favorable when the moments of a pair of islands are aligned, so that one is pointing into the center of the vertex and the other is pointing out, while it is energetically unfavorable when both moments are pointing inward or both are pointing outward. Therefore, the system is expected to be frustrated because for a particular configuration obeying the icelike rule (three-in/three-out), from the 15 possible pairs of islands in a vertex, only 9 can minimize the energy. For the sake of comparison, we remember that in the square spin ice there are 6 pairs at each vertex and only 4 can minimize the energy when the ice rule is considered.

Each vertex of the system has 64 configurations distributed in 8 different topologies (let us recall that the square lattice has only 16 configurations distributed in 4 topologies). In Fig. 2 we show these configurations and topologies, grouped by increasing energy. Types 1, 3, and 5 obey the three-in/three-out "ice rule," and analogously to the square lattice, they are energetically split. The remaining types of vertices shown in Fig. 2 possess monopole-like magnetic charges. These correspond to the flip of one, two, or even three spins in a particular vertex. For instance, types 2, 4, and 6 are monopoles with single charges (with four-in/two-out or two-in/four-out configurations), while types 7 and 8 are doubly (five-in/one-out or one-in/five-out) and triply (six-in or six-out) charged monopoles, respectively. There are, therefore, three different classes of monopoles with single charge and only one class of doubly and triply charged.
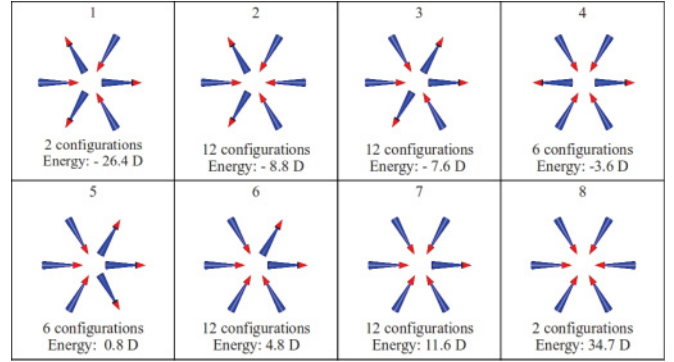

FIG. 2. (Color online) The 64 possible vertices, grouped by increasing energy (left to right) in 8 topologies. Vertices type 1, 3, and 5 satisfy the three-in/three-out ice rule, while vertices type 2, 4, and 6 are single magnetic charges. Vertices type 7 and 8 are double and triple charged vertices, respectively.

At this point, a fundamental difference between the ASSI and the ATSI appears: while in the ASSI all vertices violating the ice rule have more energy than the vertices that satisfy it, for the ATSI this is not true. In an energy scale we have type 1 vertices, which satisfy the ice rule, followed by type 2 vertices, which have four-in/two-out or four-out/two-in spins and of course do not satisfy the ice rule. Indeed, type 2 vertices have less energy than type 3 and 5 vertices, which have three spins in, three spins out. In addition, type 4 vertices, which do not satisfy the ice rule, have less energy than type 5 vertices. From this perspective, one should expect many differences in the collective behavior of the ATSI and ASSI, for example in the lowest energy excitations and in the thermodynamic properties; but as will be shown soon, they are much more similar than expected.

Going beyond the study of a single vertex, we have checked by a simulated annealing process (a Monte Carlo simulation where the system's temperature is slowly decreased)[14] that the system's ground state is indeed composed only by type 1 vertices, as can be expected by the vertex energies shown in Fig. 2. Details of the Monte Carlo procedure, including lattice sizes, etc., are given in Sec. V. A sketch of the system in its ground state is shown in Fig. 1.

III. LOWEST ENERGY EXCITATIONS

The lowest energy excitation that can be obtained above the ground state is achieved by flipping one spin creating two type 2 vertices, as shown in Fig. 3(a). This process has an energy cost of approximately $66D$. The second lowest energy state is obtained by flipping a plaquette [Fig. 3(b)] and has an energy cost of approximately $77D$. In this case, three type 3 vertices are created.

Of particular interest is the case in which after flipping one spin, which creates two type 2 vertices, more spins are flipped (without further violation of the ice rule) in order to separate them. As can be seen in Fig. 3(a), to move a excitation to the right side, keeping the neutrality (three-in/three-out) in between, we have three options: flip the spins 1, 2, or 3. By symmetry, it is clear that flipping spins 1 or 3 has the same effect in the system and generates the configuration shown in
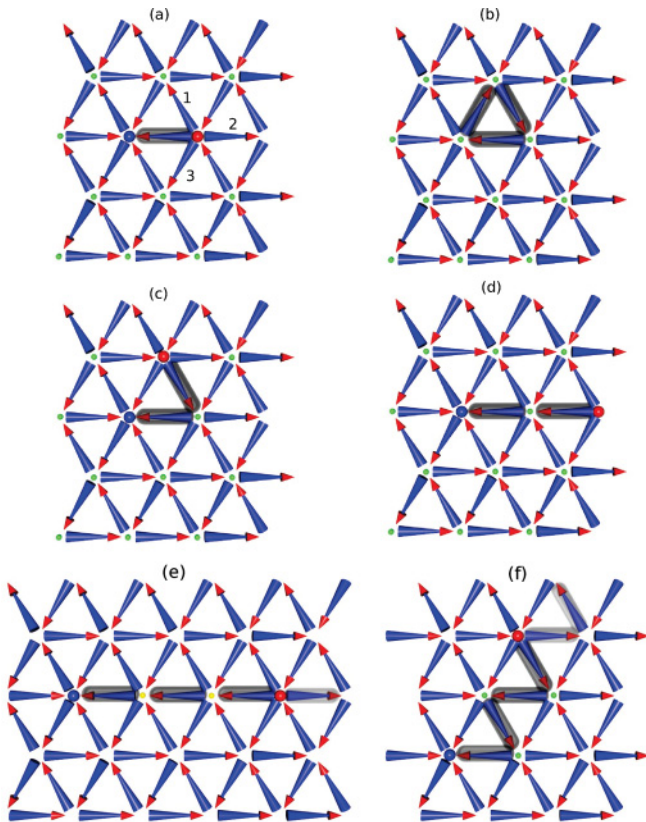
FIG. 3. (Color online) (a) Flipping the spin marked in gray results in a monopole-antimonopole pair (big dots). This is the lowest energy excitation of the system. By flipping spins 1, 2, or 3, the configurations of (c) and (d) can be obtained. (b) The second lowest energy state, which is obtained by flipping the marked spins. (c) The third lowest energy state. By repeating this process, a sawtooth-like string can be formed. (d) The fourth lowest energy state, obtained by flipping the marked spins. (e) A linear string path, where spins marked in dark gray were flipped. By flipping the spin marked in light gray, the monopoles are separated by one more lattice spacing. Type 5 vertices that compose the string are marked with small (yellow) dots. (f) A sawtooth string, where spins marked in dark gray were flipped. By flipping the spins marked in light gray, the monopoles are separated by one more lattice spacing while the string length increases by two lattice spacings. Type 3 vertices that compose the string are marked with small (green) dots.

Fig. 3(c), where a type 3 vertex is created. On the other hand, if spin 2 in Fig. 3(a) is flipped, the configuration shown in Fig. 3(d) is formed, which comprises the appearance of a type 5 vertex. As expected, the configuration in Fig. 3(c) has less energy than the configuration of Fig. 3(d). While the former costs about $91D$ to be created, the latter needs an energy about $123D$. This process can be repeated in order to separate type 2 vertices, and the energy of each configuration can be readily obtained in such a way that we can get the potential energy of the system as a function of the distance between the vertices. Therefore, we have used the same methods of Refs. 14 and 15 to determine the potential that better describes the interaction between type 2 vertices. Our results are very similar to those obtained in these references, such that the potential reads

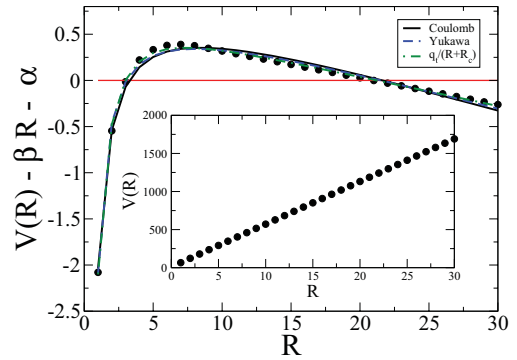$$V(R) = q_t/R + b_t X(R) + c_t, \qquad (2)$$

FIG. 4. (Color online) Inset: Potential energy as a function of the distance (R) between two single charged monopoles separated by a straight string. Outset: The black dots represent the potential minus the linear contribution obtained by fitting $\beta R + \alpha$ to it. The lines are the best nonlinear curve fits of the potential according to the functions ($q_t/R + b_t R + c_t$) Coulomb, [$q_t \exp(-\kappa R)/R + b_t R + c_t$] Yukawa, and $q_t/(R + R_c) + b_t R + c_t$ minus $\beta R + \alpha$.

where R is the distance between the monopoles and $X(R)$ is the string length.

Before showing numerical results, some points deserve further explanation. At first glance, the potential function seems to be linear (see the inset of Fig. 4). However, after subtracting from the potential the linear contribution (see Fig. 4), one can see that a diverging contribution to the potential for small enough distances must be added to the potential. Among the many possible functions that could be used, we found that the addition of a Coulombian term (q_t/R) to the potential is the best way to describe the ASSI and ATSI data using a function with only three parameters. For the sake of comparison, the χ^2/d.o.f. is about 0.3 for the pure linear fit and about 6×10^{-4} for the potential of Eq. (2). Besides that, as can be seen in Fig. 4, the potential of Eq. (2) better describes the data. As is well known, one should be very careful when doing a nonlinear curve fitting, especially when the fitted function has many parameters, such that the use of functions with more than three parameters was avoided. This is the reason why we have opted to describe the excitations by means of Eq. (2). We have also tested other functional forms instead of the Coulomb one, especially the Yukawa potential [$q_t \exp(-\kappa R)/R$] and the function $q_t/(R + R_c)$, both with four parameters. Using the Yukawa potential, we found approximately the same values for the constants (q_t, b_t, and c_t) and the χ^2/d.o.f. diminished by less than one order of magnitude. The use of the $q_t/(R + R_c)$ diminished the χ^2/d.o.f. by about one order of magnitude. Nevertheless, the fit convergence is highly dependent on the initial values, such that for all purposes we are considering Coulombian interactions between the monopoles. It is worth noticing that the values shown here are approximate results that depend on the number of points used in the nonlinear fit. Differences up to 20% in q_t may be expected.

When single-charged monopoles (type 2 vertices) are separated in a straight line by a straight string composed of type 5 vertices only [see Fig. 3(e)], the constants in the potential are $q_t^l = -3.5Da$, $b_t^l = 56D/a$, and $c_t^l = 13D$. The monopoles can also be separated in a straight line by creating only type 3 vertices [see Fig. 3(f)], such that the string has a

sawtooth shape. In this case, the constants are $q_t^s = -3.9Da$, $b_t^s = 25D/a$, and $c_t^s = 46D$, where the string length X is related to the charge distance, R, by $X = 2R$. The huge difference in the string tension in these situations can be easily understood by recalling that type 3 vertices have less energy than type 5 vertices. It is important to stress that the string in this system is energetic, observable, and unique, in the sense that it is composed of type 3 or type 5 vertices on a background of type 1 vertices. In addition, the value of q_t is almost the same of that found in the square spin ice ($-4Da \leqslant q_s \leqslant -3.4Da$),[15] while the string tension is about six times higher when the string is composed of type 5 vertices only and about two times higher when the string is composed of type 3 vertices ($b_s \sim 10D/a$). The difference in the string tension for the shapes considered indicates that there is a huge anisotropy in the system.

IV. GROUND-STATE CONSIDERATIONS

From an experimental point of view, the achievement of the system's ground state is an important step toward the study of monopole physics. Considering the ATSI, we believe that two different approaches can drive the system to its ground state, or at least to a state close enough to it. The first one is the same approach used by Morgan *et al.*[16] to study the ASSI. In their work, they studied the as-grown system and found the appearance of ground-state domains with sparse excitations that follows Boltzmann statistics. Considering, for instance, the same island sizes and lattice spacings used by Morgan *et al.*,[16] we may expect the achievement of larger domains in the ATSI as compared to the ASSI since in the ATSI, the internal magnetic fields should be stronger. This is by virtue of the presence of more islands in the same area of the material. However, due to experimental difficulties, namely the resolution of the lithography process, it may not be possible to use the same sizes and lattice spacings used by Morgan *et al.*[16] However, a simpler approach can also be very efficient to drive the system to its ground state, as will be discussed in what follows.

Apply a strong magnetic field in the $-x$ direction of the sample (see Fig. 1), so that the system is driven to the magnetized state shown on the right side of Fig. 1, similarly to what happens to ASSI. However, the energetics of these magnetized configurations, and those deviating from them, are not equivalent in the ASSI and in the ATSI. While the magnetized state of the ASSI is a local minimum, since it is composed of vertices that satisfy the ice rule and any spin flip would increase the system's energy, in the ATSI the magnetized state is a kind of saddle point. The ATSI's magnetized state is composed of type 5 vertices only. If a spin in the x direction is flipped, two type 2 vertices are created, and since type 2 vertices have less energy than type 5 vertices, the system's energy diminishes. The first spin flipped in the x direction would release an energy of about $45D$. However, if a spin in any other direction is flipped, the energy of the system increases since two type 6 vertices are created (remember that type 6 vertices are more energetic than type 5 vertices). If the first spin flipped is not in the x direction, the system's energy increases by about $10D$. We may thus expect that, after applying a strong field in the $-x$ direction, another field

applied in the $+x$ direction would induce the formation of type 2 vertices. Once formed, these vertices can be separated by the creation of type 1 vertices reducing even more the system's energy. In this process, only spins in the x direction (the field direction) are expected to flip. This process would occur in such a way that monopole-like excitations are created above a given state (which is not the ground state, such that the monopole terminology does not seem to be appropriate) and induced by the presence of the magnetic field to move along the field direction. Note, however, that south poles (with four-in/two-out) in this situation would move in the field directions instead of moving against the field, as would be expected by analogy with basic electrostatics. If we restrict our analysis to vertex energy only, we may see that spins that are not in the x direction are not expected to flip at all since the vertices that would be created in such a process (type 6) are much more energetic than the other vertices present in the system (types 1, 2, and 5). Even in the presence of a relatively strong disorder, the energy needed to flip a spin that is not in the x direction seems to be high enough to prevent its occurrence. However, a detailed analysis of this hypothesis is required due to the long-range character of dipolar interactions. A complete treatment of this possibility is currently in progress and will be published elsewhere.

V. THERMODYNAMICS

Knowing the ground state and the elementary excitations, the thermodynamics of the proposed system deserves attention. Despite the fact that in the artificial spin ices the moment configuration is athermal, some experimental works have presented alternative methods to overcome this difficulty.[16,21] Materials with an ordering temperature near room temperature[21] are the most recent option; a reduction in the island's volume and moment through state-of-the-art nanofabrication is another, but it has not been accomplished yet. Besides that, an effective thermodynamic behavior can be obtained by using a rotating magnetic field.[22–24] Independently of the experimental difficulties, we have theoretically studied some thermodynamic properties of the proposed array. Indeed, in an earlier paper considering the ASSI, we have argued that the string should lose its tension due to entropic effects[14] (the string configurational entropy), rendering free monopoles at a temperature above a critical one, T_c. The same arguments should be valid here, such that the verification of this hypothesis is of great interest.

To study the thermodynamic properties of this system, we have used conventional Monte Carlo techniques, which are briefly presented. We have simulated lattices with size $L \times L_y$, where L_y is the largest integer resulting from $L/\sqrt{3}$, so that we have $2 \times L \times L_y$ vertices and $N_s = 6 \times L \times L_y$ spins for a given L; we have considered systems with $L = 16, 24, 32, 48, 64,$ and 80. Although it is known[25] that the introduction of a cutoff radius in the evaluation of dipolar interactions may lead to a critical behavior that does not agree with that found when full long-range interactions are considered, we have opted in this work to use a cutoff radius at eight lattice spacings. This choice is justified by our interest in the basic thermodynamic behavior of the system and not in the details of the possible phase transitions. In our Monte
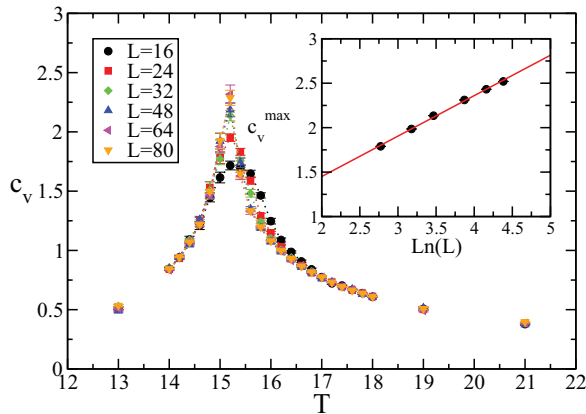
FIG. 5. (Color online) Specific heat as a function of temperature for different lattice sizes. The inset shows the specific-heat maxima as a function of $\ln(L)$. The line is a guide to the eyes.

FIG. 7. (Color online) Mean distance between single charges as a function of temperature. The inset shows the maximum mean distance as a function of $\ln(L)$. The line is a guide to the eyes.

Carlo scheme, a combination of single spin flips and loop moves was used. A loop move[26] is a random closed path of aligned spins that are flipped or not according to the METROPOLIS prescription [$p = \exp(-\Delta E/k_B T)$]. One Monte Carlo step (MCS) is the combination of N_s single spin flips and three loop moves. In most simulations, we have used 2×10^4 MCSs to equilibrate the system and 2×10^5 MCSs to take averages.

We start by presenting the results for the specific heat (see Fig. 5). We notice that the specific heat exhibits a peak at a temperature T_c approximately equal to $15D/k_B$. The amplitude of this peak increases as the system size L increases, as can be seen in the inset of the same figure, where the specific-heat maximum is plotted as a function of $\ln(L)$. Therefore, it may indicate a phase transition in the Ising universality class.[27] We have also analyzed the charge density and the average separation between monopoles and antimonopoles as a function of T. In Fig. 6, we show the density of single charges (vertices types 2, 4, and 6), ρ_1, double charges (type 7 vertices), ρ_2, and triple charges (type

8 vertices), ρ_3, as a function of temperature. It is remarkable that the density of double and triple charges is much smaller than the density of single charges.

The mean distance between monopoles and antimonopoles, S, as a function of temperature was obtained by considering only defects with unit charge. This quantity is calculated by using the method of assignment problems.[28] In our case, we would like to assign n positive charges to n negative charges for a given configuration in such a way that the sum of distances of all possible pairing will be a minimum. Note that in studying the system's thermodynamics, we are not able to determine the exact pair's energy nor which charge forms a pair with which other charge. The results are shown in Fig. 7. The average separation has a local maximum at the same temperature T_c in which the specific heat exhibits a peak ($\sim 15D$). We notice that the amplitude of this maximum also increases as the system size increases. Indeed, the maximum average separation S_m increases logarithmically with the system size L ($S_m \propto \ln L$, see the inset of Fig. 7) and hence one could expect that a certain quantity of monopoles may be almost isolated for very large arrays. For low temperatures, the average separation S does not depend on the lattice size L, while for high temperatures, this quantity has a tiny dependence on L. This picture is suggestive and indicates a different behavior of monopoles and strings at low and high temperatures.[14,19]

At this point, we should stress that the similarities between these results and the results for the ASSI of Ref. 19 are remarkable. As discussed before, one would expect many differences between those systems since some vertices that do not satisfy the ice rule have less energy than some vertices that do satisfy it. Indeed, the fact that the vertices of a string (types 3 and 5) have more energy than one kind of charge (type 2 vertices) would be expected to considerably change the system's properties, especially those concerning monopole behavior. However, the only difference that can be noticed is in the critical temperature, which is about $15D/k_B$ for the ATSI and $7D/k_B$ for the ASSI. The specific heat and magnetic charge behaviors are qualitatively the same, including the mean distance between opposite magnetic charges and their finite-size behavior. Of course, as the string in the ATSI has stronger tension, the maximum value of the mean distance
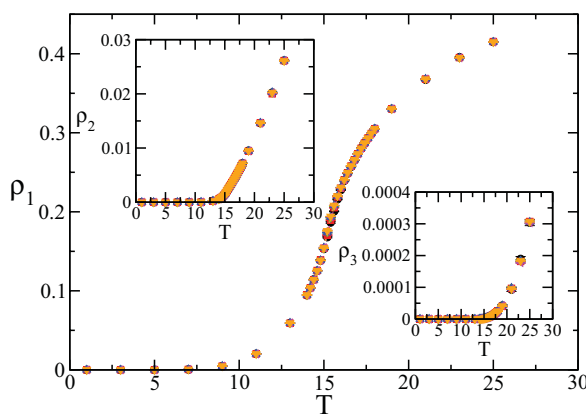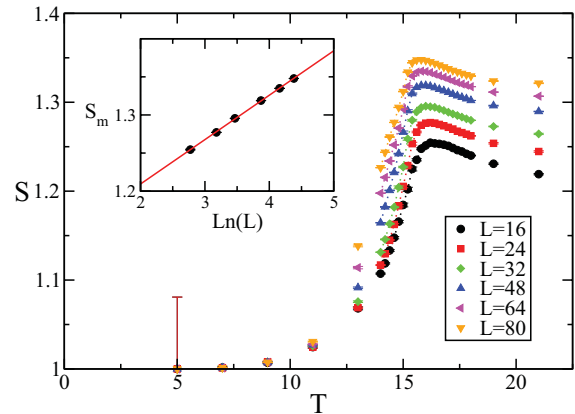

FIG. 6. (Color online) Monopole density as a function of temperature for different lattice sizes. The outer plot shows the density of single charges (ρ_1) while in the insets the density of double (ρ_2) and triple (ρ_3) charges is shown. The symbols are the same as those used in Fig. 5.

between the monopoles is smaller than that of the ASSI for the same lattice size.

VI. CONCLUSIONS

In summary, we have proposed and theoretically studied the realization of an artificial spin ice in a triangular geometry. The usual experimental difficulty to achieve the ground state of the artificial square spin ice (ASSI) should not be so dramatic for the artificial triangular spin ice (ATSI) array since a simple demagnetization protocol (similar to a hysteresis loop) will probably drive the system to its ground state, as discussed in Sec. IV (see Fig. 1). This hypothesis is under current investigation. Although there are fundamental differences between the ASSI and the ATSI, especially concerning the vertex topologies, these systems show remarkable similarities. Indeed, the lowest energy excitations of both can be described by magnetic monopole excitations interacting via a Coulombic term added by an energetic string potential; the thermodynamic behaviors are qualitatively the same. However, contrary to the ASSI, in the ATSI there are three different classes of magnetic monopoles, and much more work has to be done to completely understand if all kinds of charged vertices behave in the same way. The same applies for the different classes of three-in/three-out vertices.

Another issue that deserves further investigation is the similarity found in the monopoles' charge value. While the string tension of the ATSI can be about six times larger than that of the ASSI, the monopoles' charges have roughly the same value. Indeed, in Ref. 15 we have shown that in a modified ASSI, where a height offset is introduced between the islands in the two different lattice directions, the string tension can be reduced by a factor of about 20 and the monopoles' charge does not change appreciably. For example, the smallest value of the string tension found for the modified ASSI is about $0.59D/a$ and the highest value we found in this study is $56D/a$, which gives a difference of about two orders of magnitude. In general, we expect that the value of the string tension b will not alter the physical picture of artificial systems with different geometries; it must only change the thermodynamic quantities, and T_c should increase

as b increases (for instance, square and triangular lattices present similar thermodynamic properties but T_c is lower in the square lattice, which has smaller b). Remember that following our arguments on energy-entropy balance in ASSI,[14] we found that the effective string tension should be given by $b - \epsilon k_B T$, with $\epsilon = O(a^{-1})$. In this way, the critical temperature, the temperature at which the string loses its effective tension, is proportional to the string tension b. Of course, $T_c \to 0$ if $b \to 0$ and hence magnetic monopoles would be found free for any temperature. Besides, it is expected that smaller string tension demands a weaker field to move the monopoles. On the other hand, all monopoles' charge values are in the range $-4Da \leqslant q \leqslant -3.4Da$.[15] This observation may indicate that these charges have a kind of universal behavior while the string tension can be tuned by modifying the system's geometry. In addition, it is expected that when controlling the monopole motion, spin ice systems could be used for several practical applications. Indeed, the ability to design systems with desired string tension, with regard to the field necessary to move a charge, would aid in the development of new devices. The main challenge should then be to find geometries in two dimensions (or even in three dimensions)[15,17] in which $b \sim 0$, making the control of monopole excitations experimentally feasible by means of externally applied magnetic fields. Of course, a great deal of effort must be made in order to verify the validity and applicability of these assumptions.

Another prospect for future investigation is the search for a three-dimensional natural version of this system, a hypothetical "bulk spin ice" with a three-in/three-out ice rule. In this case, the expected crystalline structure would be composed of Ising-like spins (as in $Dy_2Ti_2O_7$ and $Ho_2Ti_2O_7$) disposed in a network of linked octahedra (which represents the central intersection of two tetrahedra) in such a way that they are constrained to point along the line joining the center of adjacent octahedra.

---

*lucasmol@ufv.br

†apereira@ufv.br

‡winder@ufv.br

[1] C. Castelnovo, R. Moessner, and L. Sondhi, Nature (London) **451**, 42 (2008).

[2] T. Fennell *et al.*, Science **326**, 415 (2009).

[3] D. J. P. Morris *et al.*, Science **326**, 411 (2009).

[4] S. T. Bramwell *et al.*, Nature (London) **461**, 956 (2009).

[5] H. Kadowaki *et al.*, J. Phys. Soc. Jpn. **78**, 103706 (2009).

[6] L. D. C. Jaubert and P. C. W. Holdsworth, Nat. Phys. **5**, 258 (2009).

[7] S. R. Giblin *et al.*, Nat. Phys. **7**, 252 (2011).

[8] S. Ladak *et al.*, Nat. Phys. **6**, 359 (2010).

[9] R. F. Wang *et al.*, Nature (London) **439**, 303 (2006).

[10] J. Li, X. Ke, S. Zhang, D. Garand, C. Nisoli, P. Lammert, V. H. Crespi, and P. Schiffer, Phys. Rev. B **81**, 092406 (2010).

[11] H. Zabel, A. Schumann, W. Westphalen, and A. Remhof, Acta Phys. Pol. A **115**, 59 (2009).

[12] E. Mengotti *et al.*, Nat. Phys. **7**, 68 (2011).

[13] Y. Nambu, Nucl. Phys. **130**, 505 (1977).

[14] L. A. Mól *et al.*, J. Appl. Phys. **106**, 063913 (2009).

[15] L. A. S. Mól, W. A. Moura-Melo, and A. R. Pereira, Phys. Rev. B **82**, 054434 (2010).

[16] J. P. Morgan, A. Stein, S. Langridge, and C. Marrows, Nat. Phys. **7**, 75 (2011).

[17] G. Möller and R. Moessner, Phys. Rev. B **80**, 140409(R) (2009).

[18] G. Möller and R. Moessner, Phys. Rev. Lett. **96**, 237202 (2006).

[19] R. C. Silva, F. S. Nascimento, L. A. S. Mól, W. A. Moura-Melo, and A. R. Pereira, New J. Phys. **14**, 015008 (2012).

[20] Z. Budrikis, P. Politi, and R. L. Stamps, Phys. Rev. Lett. **105**, 017201 (2010).

[21] V. Kapaklis *et al.*, New J. Phys. **14**, 035009 (2012).

[22] X. Ke, J. Li, C. Nisoli, P. E. Lammert, W. McConville, R. F. Wang, V. H. Crespi, and P. Schiffer, Phys. Rev. Lett. **101**, 037205 (2008).

[23] C. Nisoli, R. Wang, J. Li, W. F. McConville, P. E. Lammert, P. Schiffer, and V. H. Crespi, Phys. Rev. Lett. **98**, 217203 (2007).

[24] C. Nisoli, J. Li, X. Ke, D. Garand, P. Schiffer, and V. H. Crespi, Phys. Rev. Lett. **105**, 047205 (2010).

[25] L. A. S. Mól and B. V. Costa, e-print arXiv:1109.1840 (cond.mat).

[26] G. T. Barkema and M. E. J. Newman, Phys. Rev. E **57**, 1155 (1998).

[27] *Finite Size Scaling and Numerical Simulation of Statistical Systems*, edited by V. Privman (World Scientific, Singapore, 1990).

[28] R. Bukard, M. Dell'Amico, and S. Martello, *Assignment Problems* (Society for Industrial and Applied Mathematics, Philadelphia, 2009).